



Hot and dry compound events in South America: present climate and future projections, and their association with the Pacific Ocean

Soledad Collazo^{1,2} · Mariana Barrucand^{1,3} · Matilde Rusticucci^{1,3}

Received: 14 October 2022 / Accepted: 26 June 2023 / Published online: 16 August 2023
© The Author(s) 2023

Abstract

Compound hot and dry events can cause greater impacts than those generated by individual extreme events. Understanding the physical mechanisms that lead to their development is particularly important for an early warning. The aim of this study is to assess the ability of global climate models (GCMs) to simulate hot/dry compound events in South America (SA) during the historical period 1979–2014, in comparison with observational and reanalysis datasets. Additionally, this work seeks to investigate the potential changes in these events under two future climate scenarios for the period 2065–2100. Furthermore, we analyze the spatial patterns of sea surface temperature anomalies (SSTA) in the Pacific Ocean associated with these events in tropical and extratropical SA. In the historical period, reanalysis tends to overestimate the number of hot/dry events, while the ensemble median of GCMs performs better than the individual ones. The future projections under the high emissions scenario show longer heat waves, but a low model agreement about the number of compound events in tropical SA. For southern SA, an increase in the annual frequency of compound events is projected, and more than two hot/dry events per year are expected to occur relative to the 1979–2014 baseline. Finally, we find that compound events in tropical SA are favored during the El Niño phase, even though two other SSTA patterns have gained prominence in recent years. In southern SA, hot/dry events are associated with the negative phase of the Pacific Decadal Oscillation and the La Niña phase.

Keywords Warm extremes · Droughts · ENSO · Climate change · CMIP6

✉ Soledad Collazo
scollazo@ucm.es

¹ Departamento de Ciencias de la Atmósfera y los Océanos, Facultad de Ciencias Exactas y Naturales, Universidad de Buenos Aires, Argentina (DCAO-FCEN-UBA), Intendente Güiraldes 2160, Ciudad Universitaria, Edificio 0+Infinito, 1428 Buenos Aires, Argentina

² Departamento de Física de la Tierra y Astrofísica, Facultad de Ciencias Físicas, Universidad Complutense de Madrid, Madrid, Spain

³ Consejo Nacional de Investigaciones Científicas y Técnicas, Argentina (CONICET), Buenos Aires, Argentina

1 Introduction

Dry and hot conditions are the two most important climate disasters on a global scale because of their profound impact on crops and people's lives (Coumou and Rahmstorf 2012). In many cases, these two conditions may occur at the same time or in sequence, and in the same geographic location or at multiple locations (Zscheischler et al. 2018; Raymond et al. 2020). These are commonly termed compound dry and hot events. Due to the relevance of the impact of these combined extreme weather events and the processes involved, it is of fundamental importance to define them precisely and contextualize them for their study.

Temperature and precipitation compound events have been analyzed at different scales and regions of the world (Tencer et al. 2014; Orth et al. 2016; Hao et al. 2018a, b). At the global scale, Trenberth and Shea (2005) show a strong negative correlation between mean monthly temperature and precipitation during summer across continents in both hemispheres, demonstrating that summers tend to be warm/dry or cool/wet. The authors attribute this behavior to the fact that dry conditions favor direct radiation and less cooling due to evaporation. In southern South America (SA), Rusticucci and Penalba (2000) describe an inverse relationship between temperature and precipitation during the warm season (December to April): Hot summers are associated with low precipitation, especially in northeastern and central-western Argentina, southern Chile, and Paraguay, while cool summers are associated with above-normal precipitation due to an increase in the frequency of cold fronts.

However, research on compound extremes, their changes, and their impacts in southern SA has received only limited attention so far. The South American continent, and in particular, the southeast of Brazil, has experienced over the past few decades an increase in the frequency, intensity, and duration of extremely hot/dry events (Hao et al. 2018b). Perkins-Kirkpatrick and Lewis (2020) show that significant positive trends are recorded concerning the intensity and duration of the longest heat waves per year for SA during the period 1950–2014. In addition, Cunha et al. (2019) demonstrate that most Brazilian regions experienced in the last decade the most severe droughts over the past 60 years. In a study focused on the La Plata Basin, Tencer et al. (2016) analyze extreme daily temperature and precipitation events during the period 1961–2000. Based on monthly data from three reference weather stations over central, eastern, and northeastern Argentina, Barrucand et al. (2014) show that warm and dry conditions are significantly more frequent than cold and dry conditions during the warm season in the historical period studied. More recently, Olmo et al. (2020) find that compound events of intense precipitation and extreme temperature (warm nights and cold days) present significant positive trends for some regions of southern SA, in some cases coinciding with trends in individual extremes, which respond in part to changes in the frequency of the dominant atmospheric circulation patterns.

Different mechanisms may cause the occurrence of compound dry and hot events. Some of them are climate variability modes, such as natural cycles like El Niño-Southern Oscillation (ENSO), and large-scale atmospheric circulation patterns (Seneviratne et al. 2012). ENSO is the most relevant atmospheric-oceanic mode of variability on interannual time scales, which has been shown to affect precipitation and temperature in SA (Alexander et al. 2009; Arblaster and Alexander 2012; Rusticucci et al. 2017; Collazo et al. 2021a). Results from a logistic regression model show that ENSO plays an important role in the occurrence of hot/dry compound events during the warm season in regions such as the northern part of South America, southern Africa, southeastern Asia, and Australia (Hao

et al. 2018a). For instance, the El Niño event of 2015/2016, combined with the regional warming trend, is associated with unprecedented warming and a larger extent of extreme drought in Amazonia (Jiménez-Muñoz et al. 2016).

With global warming, climate projections indicate a continued intensification of these extreme events both individually (heat waves and droughts) and, above all, in compound form (Hao et al. 2018b; Seneviratne et al. 2021). Hot/dry events have been increasing in recent decades and are projected to increase in the future across global land areas (Zscheischler and Seneviratne 2017; Zhou and Liu 2018; Wu et al. 2020). Global climate models (GCMs) have proven to be extremely important tools for simulating and understanding climate; however, there are uncertainties associated with the projections, so a common practice is to quantify the uncertainties using a set of models and scenarios. Recently, a new generation of GCMs has been developed for the Phase 6 of the Coupled Model Intercomparison Project (CMIP6). CMIP6 models prove to be capable of representing the main climate characteristics across SA in a historical period (1995–2014), even though they exhibit varying skill in the spatiotemporal distribution of precipitation and temperature at subregional scale, particularly over high latitudes and altitudes (Almazroui et al. 2021). Using Regional Climate Models, Feron et al. (2019) show that heat waves are expected to be more frequent and last longer, especially in northern SA as well as along the Pacific coastline of the Atacama Desert. Heat waves and drought would occur more frequently everywhere under all emission scenarios in the future. In total, 93–95% of the world population is projected to experience more than double the current (1980–2014) number of hot/dry events by the end of the twenty-first century (Ridder et al. 2022). Using climate model large ensembles, Bevacqua et al. (2022) show that mean precipitation trends exclusively modulate the future occurrence of hot/dry compound events over land. The role of precipitation deficits in modulating and/or amplifying extreme climate events has already been demonstrated in several studies (Oglesby and Erikson 1989; Atlas et al. 1993; Fisher et al. 2007a, 2007b; Hirschi et al. 2011; Mueller and Seneviratne 2012; Whan et al. 2015). Seneviratne et al. (2010) describe the positive feedback between dry soils and temperature. Precipitation deficits lead to dry soils and reduced evapotranspiration (ET), which results in a decrease in upward latent heat flux and an increase in upward sensible heat flux. This mechanism favors an increase in temperature and a greater evaporation demand.

To understand the mechanisms behind the occurrence of these events both in the present and future climate, it is vital that GCMs adequately represent climate variability modes and their teleconnections. Recently, Collazo et al. (2021a) evaluate the performance of GCMs in representing the joint variability between El Niño and different extreme temperature indices in southern SA in the historical period. The authors conclude that there is no single set of models with the best performances, as these vary depending on the extreme index and the season considered. Subsequently, Collazo et al. (2021b) conduct an analysis of the future projections of the relationship between El Niño and temperature extremes. However, it is noteworthy that, in general, the GCMs do not project significant correlations between these variables in the future. Recently, McGregor et al. (2022) find significant future (2081–2100) changes in mean temperature and precipitation teleconnections over approximately 50% of teleconnected regions around the world in December–February relative to 1950–2014.

The objectives of this study are to: (1) evaluate the performance of GCMs in simulating hot/dry compound events in SA in the period 1979–2014, (2) analyze the projected changes by the end of the century (2065–2100) in these events under two future climate scenarios, and (3) obtain the spatial patterns of sea surface temperature (SST) anomalies in the Pacific Ocean associated with the occurrence of hot/dry compound events in tropical (north of

20°S) and extratropical (south of 20°S) SA, both in the historical and future period. Special attention is given to the modulation exerted by ENSO on these events.

2 Data and methodology

2.1 Data

This study uses daily maximum temperature and monthly precipitation data in SA for the historical period 1979–2014 and future 2065–2100 under two warming scenarios (SSP2-4.5 and SSP5-8.5) from the Coupled Model Intercomparison Project Phase 6 (CMIP6) models available at <https://cds.climate.copernicus.eu/cdsapp#!/dataset/projections-cmip6?tab=form> in February 2022. CMIP is dedicated to providing standardized climate simulations that can be useful to different scientific communities (Meehl et al. 2007). Also, the gridded observational dataset of the Climate Prediction Center (CPC) and the ERA5 reanalysis are used as references in the historical period. CPC global daily temperature and precipitation datasets from the National Oceanic and Atmospheric Administration (Xie et al. 2007) provide daily minimum and maximum temperatures and precipitation over a 0.5° latitude–longitude grid mesh from 1979 to the present (available at <https://psl.noaa.gov/data/gridded/>, accessed Aug 2021). ERA5 is the fifth-generation reanalysis from European Center for Medium-Range Weather Forecasts (Hersbach and Dee 2016; Hersbach et al. 2020) at 0.25° spatial resolution and from 1979 to the present. In this study, ERA5 with a 0.5° resolution is used (available at <https://climexp.knmi.nl/start.cgi>, accessed Aug 2021).

Monthly Pacific Ocean SST data from HadISST, ERA5, and CMIP6 models are used to estimate anomalies for the period 1981–2010. HadISST is a combination of monthly globally complete fields of SST and sea ice concentration for 1871–2019 present on a regular 1°×1° grid (Rayner et al. 2003).

All datasets are interpolated to a common grid of 1.5°×1.5° using the bilinear remapping technique to allow comparison of the results.

2.2 Definition of hot/dry compound events

Following Ionita et al. (2021), drought conditions are defined by considering 3-month Standardized Precipitation Index (SPI3) values less than -1 . The SPI is designed to detect drought during different periods at multiple time scales. The raw precipitation data are fitted to a gamma distribution and then transformed into a normal distribution. SPI values can be interpreted as the number of standard deviations by which the observed anomaly deviates from the long-term mean. Positive values in SPI indicate greater than mean precipitation, and negative values indicate less than mean precipitation.

Heat wave episodes are identified by considering periods of at least 5 consecutive days with the maximum daily temperature (Tx) above the 90th percentile of Tx for a particular calendar day. (The 90th percentile is calculated over the 1981–2010 reference period with a 5-day moving average.) This threshold and base period are used for the definition of heat waves in both historical and future periods. To characterize heat waves, the annual frequency of occurrence, duration, and mean intensity (average temperature exceedance

above the 90th percentile during the event) are estimated using the R package *heatwaveR* (Schlegel and Smit 2018).

Finally, a hot/dry compound event is defined when a heat wave episode occurs during a dry period, i.e., the start date of the heat wave is identified and if during that month the SPI3 presents values lower than -1 , then we are dealing with the occurrence of a compound event.

2.3 Model evaluation and future projections

Comparisons are made between observed, reanalysis, and modeled data over the historical period (1979–2014). Among all the individual models available, the median of the ensemble is obtained, and its performance is also evaluated. First, we assess the ability of the models to represent the various parameters that characterize heat waves (annual frequency, mean duration, and mean intensity) in SA in the historical period, since a poor representation of these will impact the ability of the GCMs to simulate the compound events. Then, the performance of the models in representing the annual frequency of hot/dry events is analyzed.

Taylor diagrams are used for evaluation purposes (Taylor 2001). These diagrams provide a concise summary of the degree of statistical similarity between the reference data and other data sets, reporting the correlation coefficient, the standard deviations, and the centered root-mean-square error. Observed CPC data are used as a reference for comparison. CPC has been used as a reference dataset in different studies in SA (Marrafon and Reboita 2020; Blázquez and Solman 2020; Balmaceda-Huarte et al. 2021, and Reboita et al. 2022, among others).

The future period 2065–2100 is considered under the SSP2-4.5 and SSP5-8.5 scenarios. Differences in heat wave parameters and annual frequency of compound events between the future and the historical periods are estimated for the ensemble median. In addition, grid points are identified where these differences show low agreement between models, i.e., where less than 80% of the models agree on the sign of the change.

2.4 Pacific SST patterns

For this study, Pacific SST patterns associated with the occurrence of tropical and extratropical SA compound events are considered separately for each region, since there is evidence from previous studies that they respond differently. For example, El Niño is often accompanied by droughts in the Amazon and northeastern South America, but also by flooding in tropical west coast and southeastern SA (Cai et al. 2020). Furthermore, the analysis is separated into two seasons: one from October to March (ONDJFM) and the other from April to September (AMJJAS). We work on these time scales to have large and stable samples, since the extreme compound condition significantly reduces the number of cases on scales smaller than seasonal.

The 25 months with the highest number of grid points affected by compound events for tropical and extratropical SA are identified in both the 1979–2014 and 2065–2100 periods for each season. To obtain the main patterns of variability of Pacific SST anomalies associated with the occurrence of compound events in the two subregions, we apply Rotated Empirical Orthogonal Functions (REOF) using the varimax method for orthogonal rotation (von Storch and Zwiers 1999). The REOF technique aims to find patterns in an existing data set that explain the largest variance through a linear combination of the original

variables, and represents an efficient method to investigate the spatial and temporal variability of time series covering large areas (Ionita et al. 2021). Monthly SST anomalies are estimated relative to a 1981–2010 baseline. Finally, these anomalies are detrended before applying REOF to filter out the effect of global warming. The input matrix of the method contains the detrended SST anomalies (SSTDA) organized in 25 columns corresponding to the 25 months in which the compound events with the largest spatial extent are recorded, and in the rows contains the grid points located in the Pacific Ocean. Thus, the principal components (PC) are areal fields, and the REOF are time series that show the correlation between the PC patterns and SSTDA for each extended compound event. These correlations are tested by a bootstrapping technique with 10,000 repetitions. We randomly permute the values of a PC and keep the SSTDA fixed. Then, we compute the spatial correlation coefficient between the permuted field and the SSTDA associated with each extended compound event. We repeat these steps 10,000 times to obtain a distribution of correlations and estimate the *p* value from this distribution. It is worth mentioning that we perform a sensitivity study of the results considering different subsamples of compound events, and we found similar patterns.

Finally, the percentage of spatially large compound events that occurred within the 3-month moving average of the SSTDA in the Niño 3.4 region (5°N–5°S, 120–170°W) above and below the ± 0.5 threshold is estimated. This index is hereafter identified as SSTEN3.4 and serves to identify the different ENSO phases.

3 Results

3.1 Evaluation of the GCMs in the historical period

First, we focus on assessing the spatial performance of the CMIP6 models by evaluating their representation of the annual frequency of heat wave events during the historical period (Fig. 1a). There is agreement among the different datasets in presenting a maximum frequency of heat wave occurrence toward the south-central of Brazil. However, the ERA5 shows approximately twice as many events as those observed by the CPC. On the other hand, it is observed in the Taylor diagrams that the median of the multi-model ensemble exceeds the performance of the individual models. The observed heat waves have their maximum mean duration in central and northeastern Brazil, as well as along the coasts of Peru and Ecuador (Fig. 1b). ERA5 reflects the same spatial pattern, somewhat more extended toward northern SA. The individual GCMs all show very poor performances. About half of the models overestimate the duration of heat waves by more than 5 days, while the other half underestimate it (not shown). Thus, the ensemble median presents a smooth field, i.e., without very pronounced peaks. In contrast, the mean intensity of heat waves is generally well represented, with a maximum in the extratropical SA (Fig. 1c).

Next, the annual frequencies of observed and modeled hot/dry compound events in the historical period are estimated, and the Taylor diagram is used to identify the best-performing models (Fig. 2). A maximum of compound events is observed in southern Brazil, in coincidence with the higher occurrence of heat waves. However, we observed that ERA5 overestimates the occurrence of these events in tropical SA. The Taylor diagram shows a greater spread among models to represent hot/dry compound events than for heat waves, which implies higher uncertainty. Again, the ensemble median is the best performing, even though the FGOALS-g3, INM-CM4.8, and INM-CM5.0 models present a similar skill to

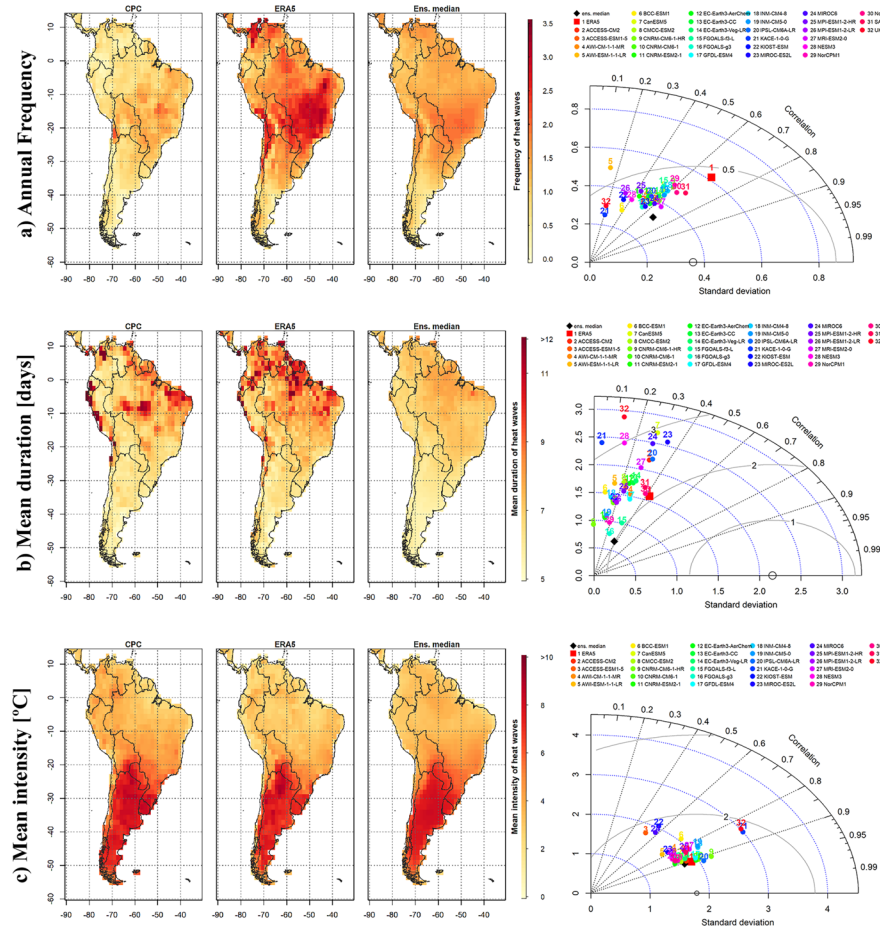


Fig. 1 Annual frequency [events per year] (a), mean duration [days] (b), and mean intensity [°C] (c) of heat waves observed by CPC (left), the ERA5 reanalysis (center), and modeled by the median CMIP6 ensemble (right) over the historical period 1979–2014. Corresponding Taylor diagrams are also shown to evaluate the performance of the models

it. In general, many models show a maximum frequency of compound events in central and northeastern SA (not shown).

3.2 Projections for the end of the century (2065–2100)

Future projections toward the end of the century (2065–2100) show an increase in the annual frequency of heat waves across SA, even though the regions with the maximum increases vary by scenario. Maximum increases occur in tropical SA under scenario SSP2-4.5 and in central SA under scenario SSP5-8.5 (Fig. 3a). Heat waves will have a longer duration in tropical SA mainly under the SSP5-8.5 scenario (Fig. 3b). Finally, the projected changes in the mean intensity of heat waves vary considerably depending on the scenario (Fig. 3c). The SSP2-4.5 scenario shows slight increases in the mean intensity of heat waves

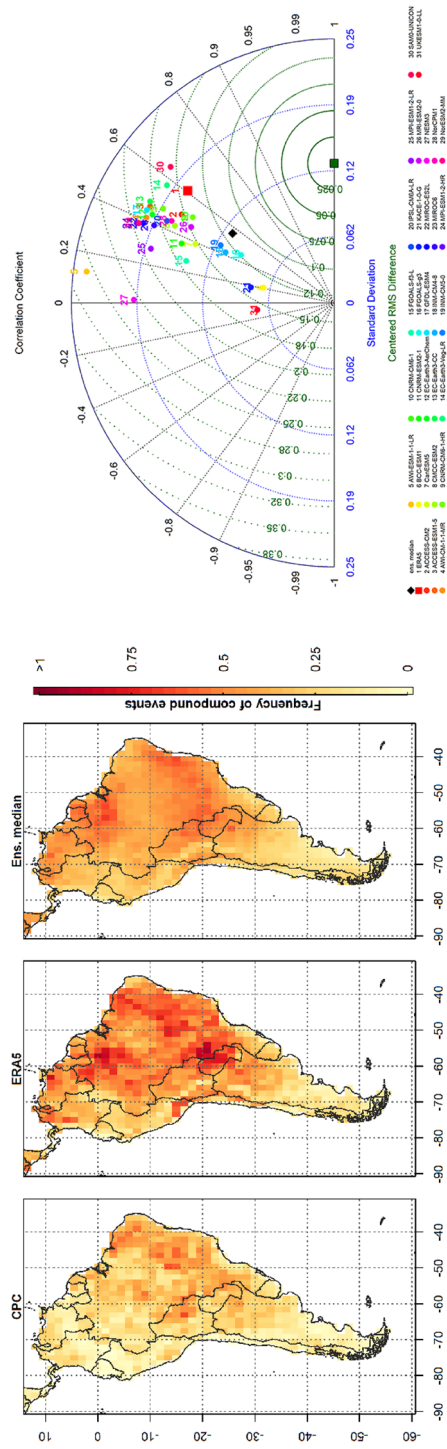


Fig. 2 Annual frequency of hot/dry compound events [events per year] observed by CPC (left), the ERA5 reanalysis (center), and modeled by the CMIP6 ensemble median (right) over the historical period 1979–2014. Corresponding Taylor diagrams are also shown to evaluate the performance of the models

in Argentina, Uruguay, and Bolivia, while it projects a weakening of heat waves in southern Brazil (although there is a low agreement between the models). This decrease could be attributed to various factors. The mean intensity of a heat wave is determined by calculating the exceedance of maximum temperature above the 90th percentile (estimated over a historical period) for all days of the heat wave, and then taking the average. With an increase in heat wave duration, there may be several days where the temperature threshold is only slightly exceeded. As a result, the average T_{max} exceedance value can be lower. Furthermore, the rising frequency of heat waves can lead to a greater variability in events, which could affect the average intensity across all events (Fig. S1). The SSP5-8.5 scenario projects an increase in the mean intensity of heat waves toward the end of the century throughout SA, with a marked maximum over central SA (Bolivia and Paraguay). Despite the different definitions, periods, and data used, Feron et al. (2019) also find that maximum increases in the duration of heat waves will occur in northern SA, while the intensity of these heat waves will not show very significant increment for the intermediate emissions scenario (RCP4.5).

As for the intensity of heat waves, the ensemble median of compound events also shows differences in the sign of the changes according to the scenario analyzed. Under the scenario SSP2-4.5, the ensemble median shows an increase in the frequency of compound events throughout SA, with a maximum over Bolivia and Paraguay. Finally, the SSP5-8.5 scenario projects a decrease in the occurrence of compound events in northern SA (although there is a large spread among the CMIP6 models) and increases in extratropical SA with a maximum over central Chile, where approximately two more hot/dry compound events are recorded per year than during the historical period (Fig. 4). The decrease in the annual frequency of compound events simulated by several models in tropical SA under the SSP5-8.5 scenario is due to the fact that the duration of heat waves increases considerably (Fig. 3b).

3.3 Pacific SST patterns associated with compound events occurrence

The spatial patterns of SSTDA in the Pacific Ocean associated with the occurrence of extensive hot/dry events during ONDJFM season in tropical SA, according to CPC, are shown in Fig. 5. It is important to note that 68% of the compound events analyzed occurred after the year 2000, indicating that these events of large spatial extent became more recurrent in recent years. These results are consistent with the warming trends observed for mean temperatures and warm extremes of maximum temperature (Parsons 2020; Collazo et al. 2022).

The first principal component (PC1) explains 43.7% of the variance of SSTDA and shows a pattern congruent with the El Niño event. PC1 presents a positive correlation with the occurrence of compound events in tropical SA with all events prior to 2005, i.e., that the El Niño phase, with its descending branch of the Walker cell over the Amazon, inhibits precipitation and favors droughts and elevated temperatures. Between 2005 and 2014, some compound events in tropical SA occurred under other ENSO phases, and the other patterns are observed to become more relevant. PC2 displays warming in the central equatorial Pacific which is consistent with El Niño Modoki (Ashok et al. 2007; Behera and Yamagata 2018). This PC presents a strong correlation with the SSTDA associated with the compound events between 2009 and 2012. Note that PC3 is congruent with a PDO pattern in its negative phase, so the spatially extensive hot/dry events over tropical SA during 2007 and 2008 occurred under this phase of the PDO. Among the 25 events with

Fig. 3 The difference in annual frequency [events per year] (a), mean duration [days] (b), and mean intensity [°C] (c) of heat waves between the values projected toward the end of the century (2065–2100) and those simulated for the historical period (1979–2014) for the median CMIP6 ensemble. For future projections, SSP2-4.5 (left) and SSP5-8.5 (right) scenarios are considered. The diagonal lines indicate low model agreement where less than 80% of models agree on the sign of change

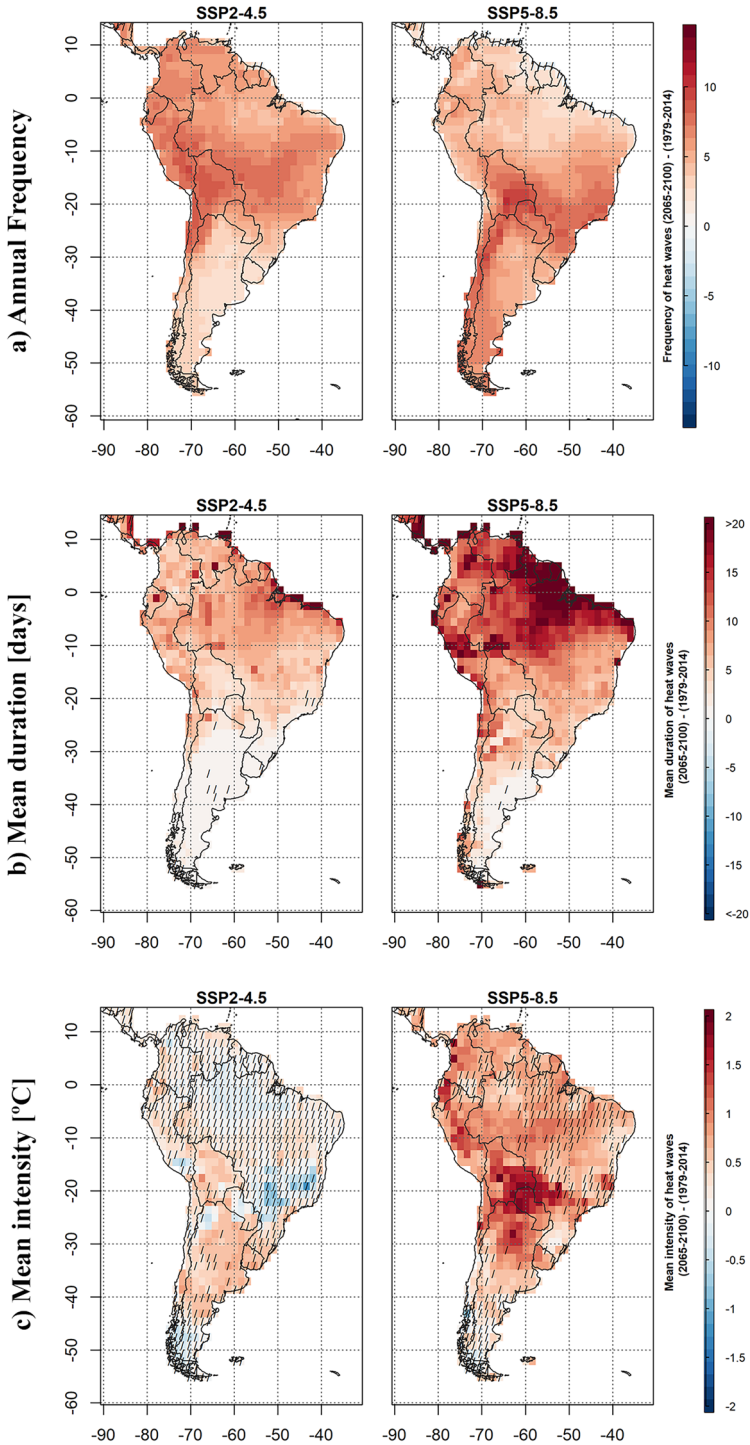
the largest spatial extent detected in tropical SA, only those occurring in 2007 and 2008 took place during a La Niña event. The negative phase of the PDO and La Niña mutually reinforces each other, leading to droughts in central-eastern SA (Wang et al. 2014; Silva et al. 2020). The effect of ENSO on dry–wet changes varies with the phase of PDO (Wang et al. 2014). When PDO and ENSO occur simultaneously, ENSO-induced dry–wet changes are amplified compared to the standard pattern. However, if out of phase, these variations can weaken or even disappear. PC4 shows, in general, little association with the compound events (except for events occurring in 2012 and 2013) and explains only 5.8% of the SSTDA variance.

The occurrence of compound events in extratropical SA during ONDJFM season is associated with the SSTDA patterns shown in Fig. 6. Analogous to what was found for tropical SA, 68% of the hot/dry events of large spatial extent in extratropical SA occurred in the present century. PC1 presents a pattern consistent with a negative phase of the PDO. Between 2008 and 2012, it is observed that most of the compound events are directly associated with the occurrence of a negative phase of the PDO. Moreover, it is observed that events occurring in the last two years of the period show strong positive correlations with PC2. This second pattern shows two main anomaly centers in the North Pacific, while in the equatorial Pacific warmer conditions are observed west of 200°E and cooler to the east. The third pattern shows two anomaly centers, one in the north-central Pacific and the other south of Australia. This pattern is dominant in the compound events that occurred during 1985/86. Finally, PC4 presents a cooling pattern in the central equatorial Pacific and shows, in general, positive associations with the occurrence of hot/dry events up to 2009. Associated with this, Fig. 7 shows that 60% of the events occurring in the extratropical SA happened with an SSTEN3.4 index below -0.5 °C. La Niña events tend to inhibit precipitation in southeastern SA due to the propagation of Rossby waves from the Pacific Ocean (Cai et al. 2020).

For the AMJJAS season, PC patterns explain a lower percentage of the SSTDA variance associated with the occurrence of extensive hot/dry events in both SA subregions (Figs. S2 and S3). Figure 7 shows that during this six-month period more than 60% of the spatially extensive hot/dry compound events occurred during a neutral ENSO phase.

Similar PCs patterns are obtained considering the ERA5 reanalysis for both subregions for ONDJFM season. Larger differences have been found in AMJJAS season, as there are no such predominant patterns.

Finally, to evaluate the ability of the GCMs to represent the Pacific Ocean patterns linked to the occurrence of extensive hot/dry events in SA, we focus on those models with the best performance at representing the annual frequency of these events. One of the models considered is INM-CM5.0; however, the patterns obtained are far from the observation in the historical period (not shown). Previous studies show that the INM-CM5.0 model presents difficulties in representing Pacific SST anomalies and ENSO (Coats and Karnauskas 2017; Seager et al. 2019; Hou and Tang 2022). Therefore, this model could be correctly representing the annual frequency of compound events in SA for the wrong physical and dynamic reasons.



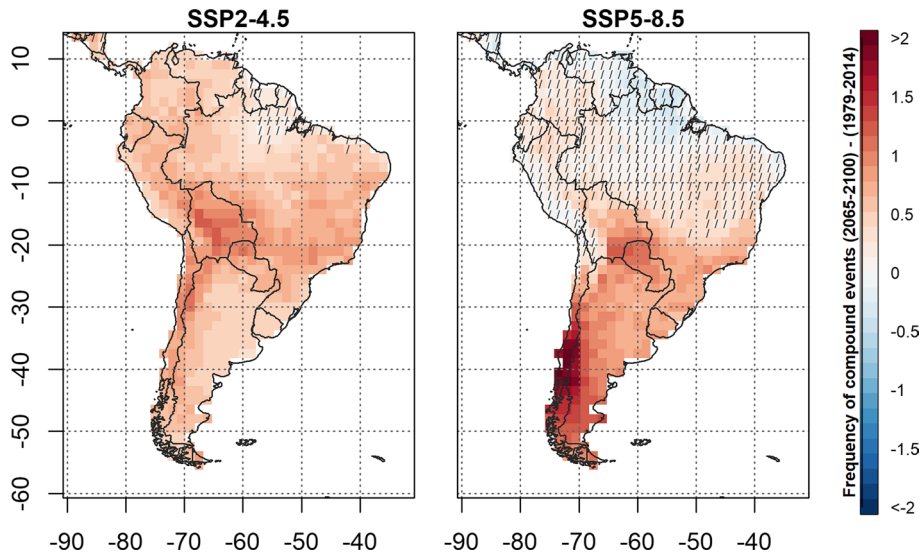


Fig. 4 The difference in the annual frequency of hot/dry compound events [events per year] between the projected values toward the end of the century (2065–2100) and those simulated for the historical period (1979–2014) for the median CMIP6 ensemble. For future projections, SSP2-4.5 (left) and SSP5-8.5 (right) scenarios are considered. The diagonal lines (*l*) indicate a low agreement of the models where less than 80% of them agree on the sign of the change

The CNRM-CM6-1 model stands out as one of the most reliable models in capturing compound events, and it also performs well in representing ENSO (Hou and Tang 2022). Therefore, we chose this model to derive the SSTDA patterns for our analysis. Additionally, we have restricted our analysis to the ONDJFM station because the first observed PC for both tropical and extratropical SA shows a higher explained variance than the AMJJAS station (Figs. 5, 6, S2, S3). The PCs patterns associated with the occurrence of hot/dry events in tropical SA estimated from CNRM-CM6-1 are shown in Fig. 8. Similar to the observed PC1 (Fig. 5), the model successfully captures the primary mode of variability, with equatorial Pacific warmings that resemble those seen during an El Niño phase. However, the SSTDA tends to be weaker, and the percentage of variance explained is lower in the simulated pattern. PC2 and PC3 of CNRM-CM6-1 largely capture the observed ENSO Modoki and PDO negative phase patterns, respectively. Finally, there are large differences between observed and simulated PC4 mainly in the North Pacific, even though it should be noted that this fourth pattern explains little variance (less than 8%).

For the compound events simulated by CNRM-CM6-1 in extratropical SA, the associated SSTDA patterns are shown in Fig. 9. The simulated PC1 shows a pattern more similar to a Modoki Niño, which was not identified as one of the main modes of variability observed. Moreover, none of the simulated patterns resembles a negative phase of the PDO, previously distinguished as the dominant mode of variability. In summary, the observed and simulated PCs (Figs. 6 and 9) show greater differences with respect to the previous comparison for the patterns associated with compound events in tropical SA. This could indicate that CNRM-CM6-1 manages to adequately simulate the Walker cell (associated with ENSO) but presents greater difficulties in representing the Rossby wave trains propagating from the equatorial Pacific to SA. Regarding this, Voltaire et al. (2019) found an underestimated teleconnection with ENSO at decadal timescales in this climate

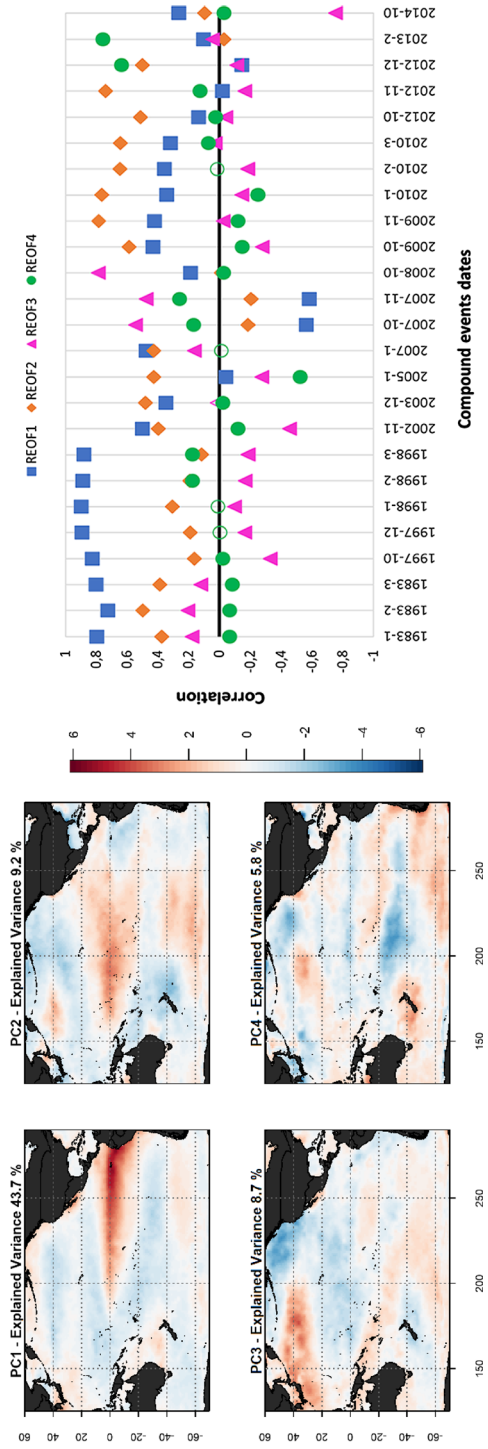


Fig. 5 Principal components (left) and REOF (right) of the observed sea surface temperature anomalies associated with the occurrence of extensive hot/dry compound events between October and March in tropical South America. Significant correlations at 1% in solid points

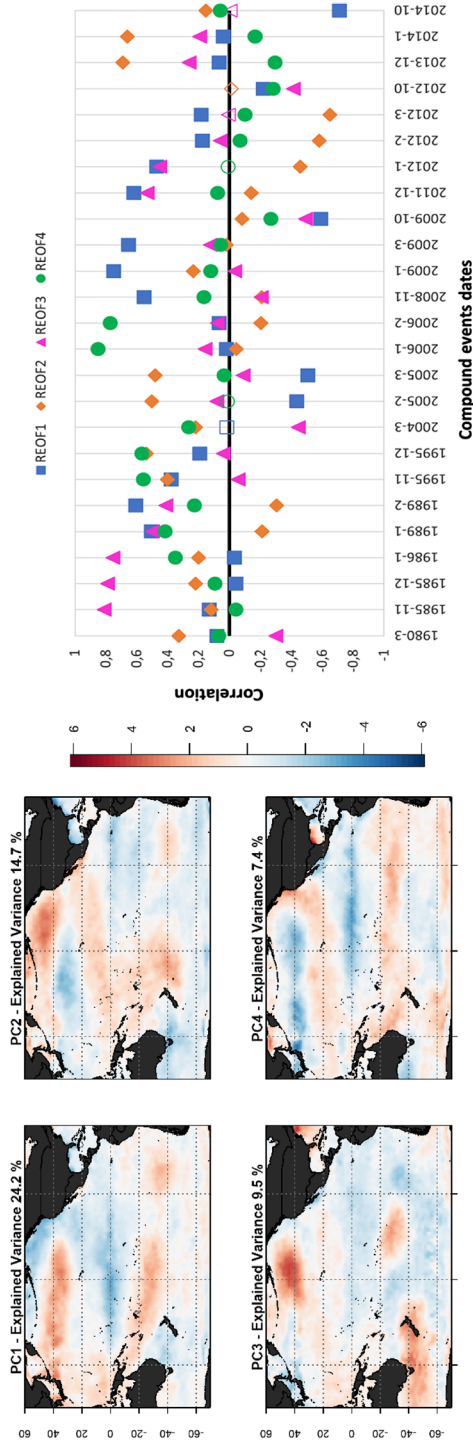


Fig. 6 Principal components (left) and REOF (right) of observed sea surface temperature anomalies associated with the occurrence of extensive hot/dry compound events between October and March in extratropical South America. Significant correlations at 1% in solid points

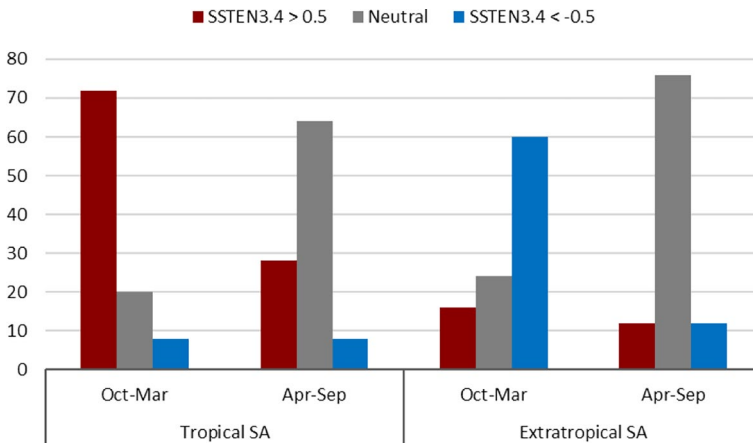


Fig. 7 Percentage of hot/dry compound events of greater spatial extent in each of the subregions that occurred under the different SSTEN3.4 thresholds

model, which has also been observed in the previous version of the model by Nidheesh et al. (2017).

The reliability of the simulated patterns toward the end of the century will be higher for the PCs associated with the occurrence of compound events in tropical SA, since it was observed that they can be simulated correctly in the historical period. This is not the case for extratropical SA hot/dry events. The first four patterns simulated by CNRM-CM6-1 under the intermediate scenario, SSP2-4.5, explain slightly more than 55% of the variance of SSTDA in tropical SA (Fig. 10). Comparing the simulated PCs for the historical and future periods associated with compound events in tropical SA, we find that both PC1s show a warming in the equatorial Pacific, even though the percentage of variance explained by this pattern would tend to decrease in the future (Fig. 10). The ENSO Modoki is represented in PC3, even though there appears to be a shift in the phase that favors hot/dry events toward the future. Finally, both phases of the PDO (PC4) would favor the occurrence of compound events in tropical SA.

4 Discussion and conclusions

Studying the projected changes in the occurrence of extreme hot/dry compound events toward the end of the century is essential to take adaptation measures, as their impacts affect a large number of socioeconomic sectors. First, an evaluation of the performance of models over a historical period must be carried out to determine whether they are capable of capturing the observed climate. The comparison between the datasets (CPC, ERA5, and CMIP6 models) reveals important differences between them. In particular, it is found that ERA5 tends to overestimate the occurrence of heat waves as well as compound events, while the CMIP6 ensemble median performs better than the individual models. In general, the observed and modeled datasets agree in showing a maximum frequency of heat waves in southern Brazil in the historical period (1979–2014). The observed heat waves have their maximum mean duration in central and northeastern Brazil, as well as on the coasts of Peru and Ecuador, while the maximum intensity occurs in southern SA. The individual

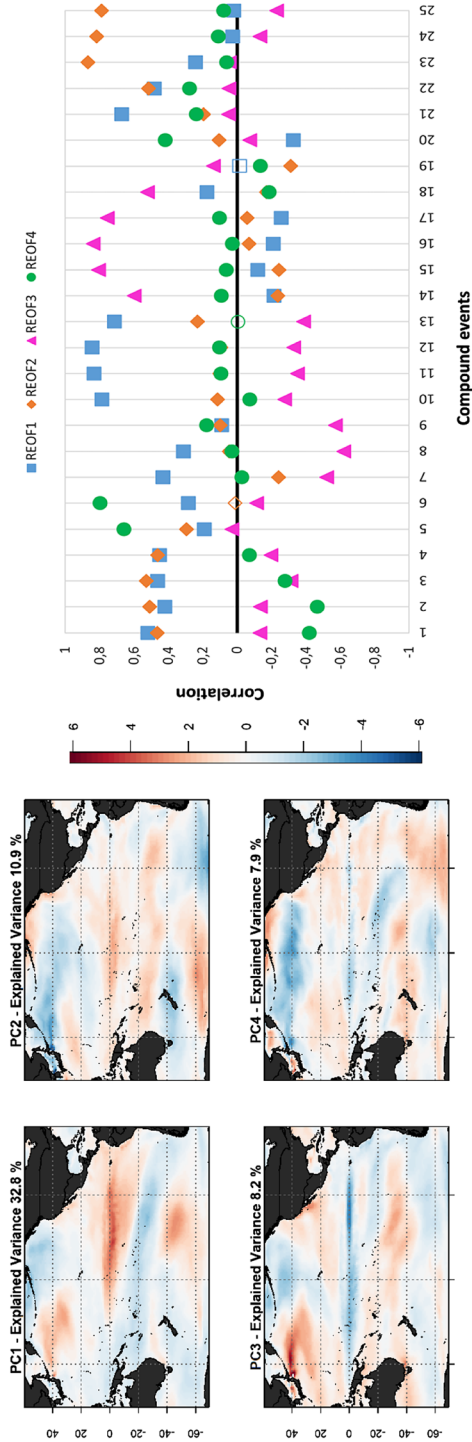


Fig. 8 Principal components (left) and REOF (right) of sea surface temperature anomalies of CNRM-CM6-1 model associated with the occurrence of extensive hot/dry compound events between October and March in tropical South America in the historical period (1979–2014). Significant correlations at 1% in solid points

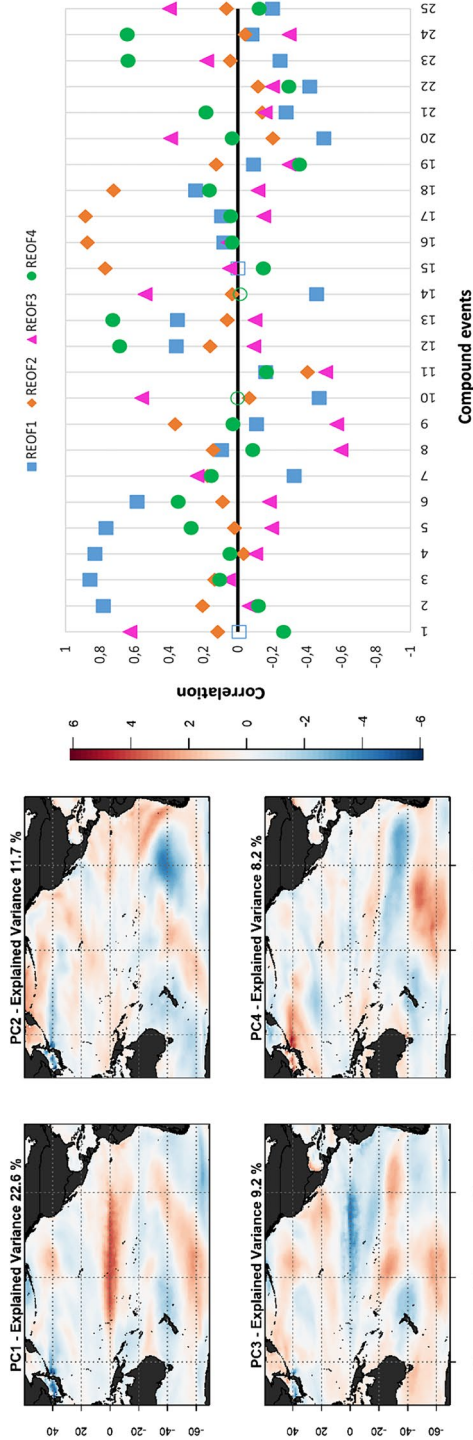


Fig. 9 Principal components (left) and REOF (right) of sea surface temperature anomalies of CNRM-CM6-1 model associated with the occurrence of extensive hot/dry compound events between October and March in extratropical South America in the historical period (1979–2014). Significant correlations at 1% in solid points

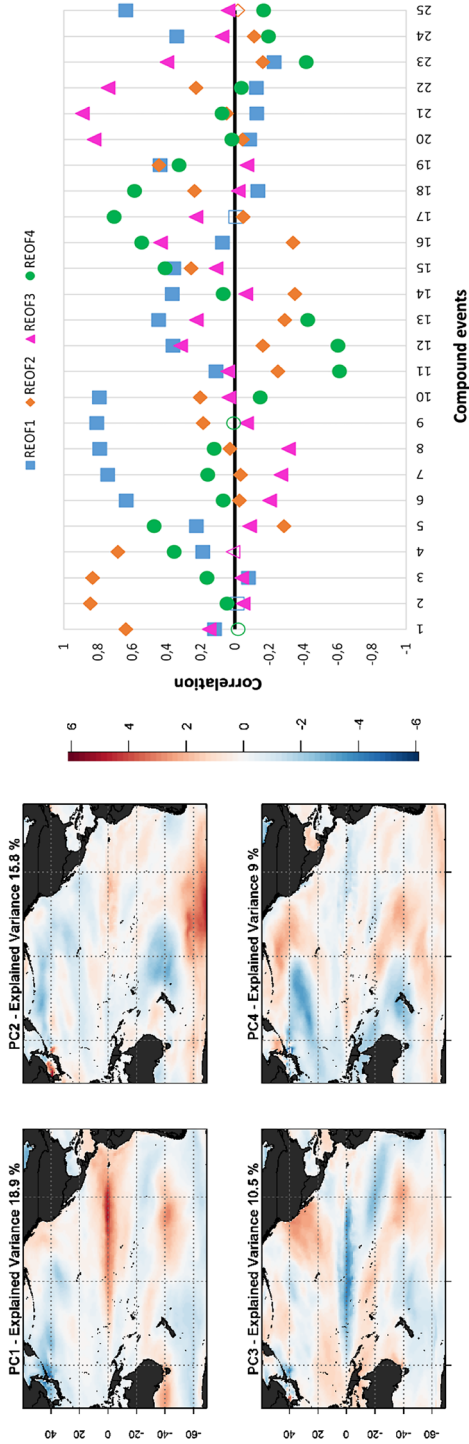


Fig. 10 Principal components (left) and REOF (right) of sea surface temperature anomalies of CNRM-CM6-1 model associated with the occurrence of extensive hot/dry compound events between October and March in tropical South America during the future period (2065–2100) under SSP2-4.5 scenario. Significant correlations at 1% in solid points

GCMs present in all cases very poor performances in the simulation of heat wave duration, while intensity is better represented. The representation of the annual frequency of hot/dry events shows a wider spread among the CMIP6 models, even though several models present two frequency maxima: one in the north of Brazil and another in the south. Among the individual models and according to a Taylor diagram, we found that FGOALS-g3, INM-CM4-8, and INM-CM5-0 presented the best performances in the simulation of compound events, being similar to the skill of the ensemble median, even though an analysis of the circulation associated with the occurrence of these events is required to determine if they represent the atmospheric and oceanic dynamics correctly. On the other hand, the worst performers are UKESM1-0-LL, NESM3, AWI-ESM-1-1-LR, BCC-ESM1, and KACE-1-0-G. Finally, we found that these compound events are more frequent in the ONDJFM season, according to the CPC and reanalysis data (not shown).

Regarding projections toward the end of the century (2065–2100), SSP2-4.5 and SSP5-8.5 scenarios show an increase in the frequency and duration of heat waves. In particular, in northern SA at the end of the century under the SSP5-8.5 scenario, the heat wave condition (defined here as 5 consecutive days above the 90th percentile estimated in the 1981–2010 reference period) constitutes the “new climate normal” since the events will tend to extend for more than 20 days. On the other hand, changes in the mean intensity of heat waves present low agreement between models (less than 80%), mainly in Brazil and southern SA, for both sceneries. These uncertainties, associated with the low agreement between models, can also be observed in the simulation of hot/dry events in the tropical regions of SA for the most extreme scenario (SSP5-8.5). There is agreement among models in projecting a drying of the Amazon in the future (Parsons 2020; Almazroui et al. 2021), which will favor the occurrence of longer-duration heat waves. Therefore, the number of events may not undergo major modifications, but their characteristics may change, i.e., they may be longer.

For extratropical SA, both scenarios show an increase in the frequency of compound events, which is higher for the SSP5-8.5 scenario. These changes projected by the CMIP6 models for the end of the twenty-first century would imply that the people living in central Chile would be exposed to approximately two more hot/dry episodes per year relative to the 1979–2014 baseline. Consistent with Ridder et al. (2022), the regions of Chile and southern Argentina with the lowest number of warm/dry episodes in the period 1980–2014 (1 episode every two to four years) are expected to experience these compound events even more frequently than the regions with the highest number of hot/dry events in the historical period.

Another objective of the present work is to obtain the main Pacific SSTDA patterns associated with the occurrence of compound events. This type of analysis allows a better understanding of the physical processes involved. The results of this work show that tropical SA compound events are favored during the El Niño phase, even though in the last years of the historical period two other SSTDA patterns have gained relevance: The first one is characterized by warm conditions in the central Pacific and cold anomalies in the South American coasts, and the second one is the PDO pattern in its negative phase. The cause of this temporal variation of the correlations with the patterns requires a more detailed study on possible changes in the associated atmospheric and oceanic circulation. Some studies showed that Modoki activity (anomalous warming events in the central equatorial Pacific) has been increasing in frequency in the last decades (Ashok and Yamagata 2009; Yeh et al. 2009). Furthermore, this central Pacific El Niño has been associated with unprecedented warming and extreme drought in Amazonia during the event of 2015/2016 (Jiménez-Muñoz et al. 2016).

In extratropical SA, the occurrence of compound events is related to the negative phase of the PDO and with the La Niña phase. Note that the El Niño phase suppresses precipitation in tropical SA due to the descending branch of the Walker cell (Marengo and Espinoza 2016), while the La Niña phase inhibits precipitation in the southeastern SA due to teleconnections. Furthermore, Reboita et al. (2021) found that in the austral spring the negative phase of the PDO is associated with dry conditions in a northwest–southeast band from northern SA to southeastern Brazil, and in the southern part of the continent. For the austral summer, the authors found negative precipitation anomalies in eastern Brazil and central Argentina linked to this phase of the PDO.

The CNRM-CM6-1 model manages to represent the SSTDA patterns associated with the occurrence of hot/dry events in tropical SA in the historical period (1979–2014), while for extratropical SA events the performance is low. Although there have been improvements with successive CMIP projects, GCMs still struggle to adequately represent climate variability modes, such as ENSO or PDO. Historically, models show ENSO-related equatorial Pacific sea surface temperature biases that extend too far westward, and the associated atmospheric teleconnections are too weak (Fasullo 2020). Furthermore, the PDO simulated by the models has a stronger tropical expression than is revealed by observations. This reduces their reliability in their future projections. In the patterns projected by CNRM-CM6-1, some hints of ENSO and PDO can be identified as a signal linked to the occurrence of compound extremes in tropical SA, but the explained variance of the first principal component is decreased. Under the SSP5-8.5 high-emission scenario, McGregor et al. (2022) find clear and significant ENSO teleconnection changes in DJF for the 2081–2100 period, relative to 1950–2014. These changes are most clearly seen as an eastward shift and intensification of the atmospheric response to ENSO. As for teleconnection amplifications, northern SA shows a clear teleconnection amplification that could favor drought conditions and longer heat wave events in the region. In addition, some studies found that, in the context of future global warming, there could be more El Niño Modoki events (Ashok and Yamagata 2009; Yeh et al. 2009).

Internal, unforced climate variability is a significant source of uncertainty in global climate simulations (Hawkins and Sutton 2009). The nonlinear and chaotic nature of the climate system implies that small perturbations to a given state of the system can result in different trajectories (Palmer 2005). To investigate the uncertainty arising from internal climate variability, we use 30 members of CNRM-CM6-1 with different initializations in the historical period. The uncertainties of internal climate variability on the frequency of heat waves are at most 0.3 events per year in SA, which is an order of magnitude smaller than the projected end-of-century changes in this parameter (Fig. S4). The duration of heat waves had a higher uncertainty in the north of SA, while the mean intensity had the smallest spread, being only a few decimal degrees and slightly larger in the south of SA. It should be noted that the uncertainty associated with the model's representation of the annual frequency of compound events is higher than the uncertainty due to internal variability, as evidenced by the comparison of the Taylor diagrams in Figs. 2 and S5. In other words, the internal variability can produce model performance metrics for a single climate model that span a slightly smaller range than the CMIP6 multi-model ensemble in Taylor diagram space.

When applying REOF analysis to each of the CNRM-CM6-1 realizations, it is important to consider certain properties of the methodology. REOF analysis is a statistical technique that allows for the analysis and interpretation of complex spatial and temporal patterns in data sets (Hannachi et al. 2007). However, the sign of the patterns in rotated EOF analysis is arbitrary and does not carry any inherent meaning. To assess the agreement

between the principal components obtained from each realization, Taylor diagrams are employed, providing a visual representation of the absolute spatial correlation between the patterns derived from CPC and CNRM-CM6-1 members (Figs. S6 and S8). The first principal component is the best represented by the simulations, although there is a large spread between realizations, particularly in the equatorial Pacific (Figs. S7 and S9). For the other PCs, as the percentages of variance explained do not differ considerably, it is possible that the ordering of the principal components may vary between members, which can limit the comparison.

This study represents a first step toward enhancing the understanding of hot and dry events in SA. The atmosphere is a complex system where multiple processes interact with each other in intricate ways. Although this study focuses on analyzing some of these processes, investigating the linkages with other ocean basins and atmospheric circulations is the next logical step. For instance, the Atlantic Multidecadal Oscillation (AMO) plays a crucial role in modulating temperature and precipitation in tropical SA (Flantua et al. 2016).

Supplementary Information The online version contains supplementary material available at <https://doi.org/10.1007/s11069-023-06119-2>.

Acknowledgements This research was supported by CONICET PIP 11220200100333CO from National Council of Scientific and Technical Research, Argentina; UBACyT 2018 20020170100357BA from University of Buenos Aires, Argentina; and PICT2019-2019-02933 from National Agency for Scientific and Technological Promotion, Argentina. This work was also supported by the SAFETE project, which has received funding from the European Union's Horizon 2020 research and innovation program under the Marie Skłodowska-Curie grant agreement No 847635 (UNA4CAREER). We also want to thank the ClimateDL project funded by the regional program CLIMAT-AmSud (22CLIMAT-02). Open Access funding provided thanks to the CRUE-CSIC agreement with Springer Nature. We acknowledge the Copernicus Climate Data Store for collecting and archiving the CMIP6 model output. The authors would like to thank the reviewers for their useful and helpful comments that have improved the manuscript.

Funding Open Access funding provided thanks to the CRUE-CSIC agreement with Springer Nature. This research was funded by CONICET PIP 11220200100333CO from National Council of Scientific and Technical Research, Argentina; UBACyT 2018 20020170100357BA from University of Buenos Aires, Argentina; PICT2019-2019-02933 from National Agency for Scientific and Technological Promotion, Argentina; and the SAFETE project, which has received funding from the European Union's Horizon 2020 research and innovation program under the Marie Skłodowska-Curie grant agreement No 847635 (UNA4CAREER).

Open Access This article is licensed under a Creative Commons Attribution 4.0 International License, which permits use, sharing, adaptation, distribution and reproduction in any medium or format, as long as you give appropriate credit to the original author(s) and the source, provide a link to the Creative Commons licence, and indicate if changes were made. The images or other third party material in this article are included in the article's Creative Commons licence, unless indicated otherwise in a credit line to the material. If material is not included in the article's Creative Commons licence and your intended use is not permitted by statutory regulation or exceeds the permitted use, you will need to obtain permission directly from the copyright holder. To view a copy of this licence, visit <http://creativecommons.org/licenses/by/4.0/>.

References

- Alexander L, Uotila P, Nicholls N (2009) Influence of sea surface temperature variability on global temperature and precipitation extremes. *J Geophys Res-Atmos*. <https://doi.org/10.1029/2009JD012301>
- Almazroui M, Ashfaq M, Islam MN et al (2021) Assessment of CMIP6 performance and projected temperature and precipitation changes over South America. *Earth Syst Environ* 5:155–183. <https://doi.org/10.1007/s41748-021-00233-6>

- Arblaster JM, Alexander LV (2012) The impact of the El Niño–Southern Oscillation on maximum temperature extremes. *Geophys Res Lett* 39(20):L20702
- Ashok K, Yamagata T (2009) Climate change: the El Niño with a difference. *Nature* 461:481–484. <https://doi.org/10.1038/461481a>
- Ashok K, Behera SK, Rao SA, Weng H, Yamagata T (2007) El Niño Modoki and its possible teleconnection. *J Geophys Res* 112:C11007
- Atlas R, Wolfson N, Terry J (1993) The effect of SST and soil moisture anomalies on GLA model simulations of the 1988 U.S. summer drought. *J Clim* 6(11):2034–2048. [https://doi.org/10.1175/1520-0442\(1993\)006%3c2034:TEOSAS%3e2.0.CO;2](https://doi.org/10.1175/1520-0442(1993)006%3c2034:TEOSAS%3e2.0.CO;2)
- Balmaceda-Huarte R, Olmo ME, Bettolli ML, Poggi MM (2021) Evaluation of multiple reanalyses in reproducing the spatio-temporal variability of temperature and precipitation indices over southern South America. *Int J Climatol* 41:5572–5595. <https://doi.org/10.1002/joc.7142>
- Barrucand M, Vargas W, Bettolli ML (2014) Warm and cold dry months and associated circulation in the humid and semi-humid Argentine region. *Meteorol Atmos Phys* 123:143–154
- Behera SK, Yamagata T (2018) Climate dynamics of ENSO modoki phenomena. *Oxford Research Encyclopedia of Climate Science*. <https://doi.org/10.1093/acrefore/9780190228620.013.612>
- Bevacqua E, Zappa G, Lehner F et al (2022) Precipitation trends determine future occurrences of compound hot–dry events. *Nat Clim Chang* 12:350–355. <https://doi.org/10.1038/s41558-022-01309-5>
- Blázquez J, Solman AS (2020) Multiscale precipitation variability and extremes over South America: analysis of future changes from a set of CORDEX regional climate model simulations. *Clim Dyn* 55(7–8):2089–2106. <https://doi.org/10.1007/s00382-020-05370-8>
- Cai W, McPhaden MJ, Grimm AM et al (2020) Climate impacts of the El Niño–Southern Oscillation on South America. *Nat Rev Earth Environ* 1:215–231. <https://doi.org/10.1038/s43017-020-0040-3>
- Coats S, Karnauskas KB (2017) Are simulated and observed twentieth century tropical Pacific sea surface temperature trends significant relative to internal variability? *Geophys Res Lett* 44:9928–9937. <https://doi.org/10.1002/2017GL074622>
- Collazo S, Barrucand M, Rusticucci M (2021a) Association between El Niño and extreme temperatures in southern South America in CMIP5 models. Part 1: model evaluation in the present climate. *Climate Res* 83:111–132. <https://doi.org/10.3354/cr01639>
- Collazo S, Barrucand M, Rusticucci M (2021b) Association between El Niño and extreme temperatures in southern South America in CMIP5 models. Part 2: future climate projections. *Clim Res* 85:69–90. <https://doi.org/10.3354/cr01673>
- Collazo S, Barrucand M, Rusticucci M (2022) Evaluation of CMIP6 models in the representation of observed extreme temperature indices trends in South America. *Climatic Change* 172:21. <https://doi.org/10.1007/s10584-022-03376-1>
- Coumou D, Rahmstorf S (2012) A decade of weather extremes. *Nature Clim Change* 2:491–496. <https://doi.org/10.1038/nclimate1452>
- Cunha APMA, Zeri M, Deusdará Leal K, Costa L, Cuartas LA, Marengo JA, Tomasella J, Vieira RM, Barbosa AA, Cunningham C, Cal Garcia JV, Broedel E, Alvalá R, Ribeiro-Neto G (2019) Extreme drought events over Brazil from 2011 to 2019. *Atmosphere* 10(11):642. <https://doi.org/10.3390/atmos10110642>
- Fasullo JT (2020) Evaluating simulated climate patterns from the CMIP archives using satellite and reanalysis data sets using the Climate Model Assessment Tool (CMATv1). *Geoscientific Model Dev* 13(8):3627–3642. <https://doi.org/10.5194/gmd-13-3627-2020>
- Feron S, Cordero RR, Damiani A et al (2019) Observations and projections of heat waves in South America. *Sci Rep* 9:8173. <https://doi.org/10.1038/s41598-019-44614-4>
- Fischer EM, Seneviratne SI, Lüthi D, Schär C (2007a) Contribution of land–atmosphere coupling to recent European summer heat waves. *Geophys Res Lett* 34:6. <https://doi.org/10.1029/2006GL029068>
- Fischer EM, Seneviratne SI, Vidale PL, Lüthi D, Schär C (2007b) Soil moisture–atmosphere interactions during the 2003 European summer heat wave. *J Clim* 20(20):5081–5099. <https://doi.org/10.1175/JCL14288.1>
- Flantua SGA, Hooghiemstra H, Vuille M, Behling H, Carson JF, Gosling WD, Hoyos I, Ledru MP, Montoya E, Mayle F, Maldonado A, Rull V, Tonello MS, Whitney BS, González-Arango C (2016) Climate variability and human impact in South America during the last 2000 years: synthesis and perspectives from pollen records. *Clim past* 12:483–523. <https://doi.org/10.5194/cp-12-483-2016>
- Hannachi A, Jolliffe IT, Stephenson DB (2007) Empirical orthogonal functions and related techniques in atmospheric science: a review. *Int J Climatol* 27(9):1119–1152. <https://doi.org/10.1002/joc.1499>
- Hao Z, Hao F, Singh VP, Zhang X (2018a) Quantifying the relationship between compound dry and hot events and El Niño–Southern Oscillation (ENSO) at the global scale. *J Hydrol*. <https://doi.org/10.1016/j.jhydrol.2018.10.022>

- Hao Z, Hao F, Singh VP, Zhang X (2018b) Changes in the severity of compound drought and hot extremes over global land areas. *Environ Res Lett* 13:124022
- Hawkins E, Sutton R (2009) The potential to narrow uncertainty in regional climate predictions. *Bull Am Meteor Soc* 90(8):1095–1108. <https://doi.org/10.1175/2009BAMS2607.1>
- Hersbach H, Bell B, Berrisford P et al (2020) The ERA5 global reanalysis. *Q J R Meteorol Soc* 146:1999–2049. <https://doi.org/10.1002/qj.3803>
- Hersbach H, Dee D (2016) ERA5 reanalysis is in production, ECMWF Newsletter No. 147, 7
- Hirschi M, Seneviratne SI, Alexandrov V, Boberg F, Boroneant C, Christensen OB, Formayer H, Orlowsky B, Stepanek P (2011) Observational evidence for soil-moisture impact on hot extremes in southeastern Europe. *Nat Geosci* 4:17–21. <https://doi.org/10.1038/ngeo1032>
- Hou M, Tang Y (2022) Recent progress in simulating two types of ENSO—from CMIP5 to CMIP6. *Front Mar Sci*. <https://doi.org/10.3389/fmars.2022.986780>
- Ionita M, Caldarescu DE, Nagavciuc V (2021) Compound hot and dry events in Europe: variability and large-scale drivers. *Front Climatic*. <https://doi.org/10.3389/fclim.2021.688991>
- Jiménez-Muñoz J, Mattar C, Barichivich J et al (2016) Record-breaking warming and extreme drought in the Amazon rainforest during the course of El Niño 2015–2016. *Sci Rep* 6:33130. <https://doi.org/10.1038/srep33130>
- Marengo JA, Espinoza JC (2016) Extreme seasonal droughts and floods in Amazonia: causes, trends and impacts. *Int J Climatol* 36:1033–1050. <https://doi.org/10.1002/joc.4420>
- Marrafon VH, Reboita MS (2020) Características da precipitação na América do Sul reveladas através de índices climáticos. *Revista Brasileira De Climatologia*. <https://doi.org/10.5380/abclima.v26i0.72181>
- McGregor S, Cassou C, Kosaka Y, Phillips AS (2022) Projected ENSO teleconnection changes in CMIP6. *Geophys Res Lett* 49:e2021GL097511. <https://doi.org/10.1029/2021GL097511>
- Meehl GA, Stocker TF, Collins WD, Friedlingstein P, Gaye T, Gregory JM, Kitoh A, Knutti R, Murphy JM, Noda A, Raper SCB, Watterson IG, Weaver AJ, Zhao ZC (2007) Global climate projections. In: Solomon S, Qin D, Manning M, Chen Z, Marquis M, Averyt KB, Tignor M, Miller HL (eds) IPCC, 2007 Climate Change 2007: the physical science basis. Contribution of working group I to the 4th assessment report of the intergovernmental panel on climate change. Cambridge University Press, Cambridge
- Mueller B, Seneviratne SI (2012) Hot days induced by precipitation deficits at the global scale. *Proc Natl Acad Sci USA* 109(31):12398–12403. <https://doi.org/10.1073/pnas.1204330109>
- Nidheesh AG, Lengaigne M, Vialard J, Izumo T, Unnikrishnan AS, Cassou C (2017) Influence of ENSO on the Pacific decadal oscillation in CMIP models. *Clim Dyn* 49(9–10):3309–3326. <https://doi.org/10.1007/s00382-016-3514-8>
- Oglesby RJ, Erickson DJ (1989) Soil moisture and the persistence of North American drought. *J Clim* 2(11):1362–1380. [https://doi.org/10.1175/1520-0442\(1989\)002%3c1362:SMATPO%3e2.0.CO;2](https://doi.org/10.1175/1520-0442(1989)002%3c1362:SMATPO%3e2.0.CO;2)
- Olmo M, Bettolli ML, Rusticucci M (2020) Atmospheric circulation influence on temperature and precipitation individual and compound daily extreme events: Spatial variability and trends over Southern South America. *Weather Clim Extremes* 29:100267. <https://doi.org/10.1016/j.wace.2020.100267>
- Orth R, Zscheischler J, Seneviratne SI (2016) Record dry summer in 2015 challenges precipitation projections in central Europe. *Sci Rep* 6:28334
- Palmer T (2005) Global warming in a nonlinear climate. Can we be sure? *Europhys News* 36(2):42–46
- Parsons LA (2020) Implications of CMIP6 projected drying trends for twenty-first century Amazonian drought risk. *Earth's Future* 8:e2020EF001608. <https://doi.org/10.1029/2020EF001608>
- Perkins-Kirkpatrick SE, Lewis SC (2020) Increasing trends in regional heatwaves. *Nat Commun* 11:3357. <https://doi.org/10.1038/s41467-020-16970-7>
- Raymond C, Horton RM, Zscheischler J, Martius O, AghaKouchak A, Balch J et al (2020) Understanding and managing connected extreme events. *Nat Clim Change* 10:611–621. <https://doi.org/10.1038/s41558-020-0790-4>
- Rayner NA, Parker DE, Horton EB, Folland CK, Alexander LV, Rowell DP, Kent EC, Kaplan A (2003) Global analyses of sea surface temperature, sea ice, and night marine air temperature since the late nineteenth century. *J Geophys Res* 108:4407. <https://doi.org/10.1029/2002JD002670.D14>
- Reboita MS, Ambrizzi T, Crespo NM, Dutra LMM et al (2021) Impacts of teleconnection patterns on South America climate. *Ann NY Acad Sci*. <https://doi.org/10.1111/nyas.14592>
- Reboita MS, da Rocha RP, Souza CAD, Baldoni TC, Silva PLLdS, Ferreira GWS (2022) Future projections of extreme precipitation climate indices over South America based on CORDEX-CORE multimodel ensemble. *Atmosphere* 13(9):1463. <https://doi.org/10.3390/atmos13091463>
- Ridder NN, Ukkola AM, Pitman AJ et al (2022) Increased occurrence of high impact compound events under climate change. *Clim Atmos Sci* 5:3. <https://doi.org/10.1038/s41612-021-00224-4>

- Rusticucci M, Penalba OC (2000) Interdecadal changes in the precipitation seasonal cycle over Southern South America and their relationship with surface temperature. *Clim Res* 16:1–15
- Rusticucci M, Barrucand M, Collazo S (2017) Temperature extremes in the Argentina central region and their monthly relationship with the mean circulation and ENSO phases. *Int J Climatol* 37:3003–3017
- Schlegel RW, Smit AJ (2018) heatwaveR: a central algorithm for the detection of heatwaves and cold-spells. *J Open Source Softw* 3(27):821. <https://doi.org/10.21105/joss.00821>
- Seager R, Cane M, Henderson N, Lee D, Abernathey R, Zhang H (2019) Strengthening tropical Pacific zonal sea surface temperature gradient consistent with rising greenhouse gases. *Nat Clim Chang* 9:517. <https://doi.org/10.1038/s41558-019-0505-x>
- Seneviratne SI, Corti T, Davin EL, Hirschi M, Jaeger EB, Lehner I, Orlowsky B, Teuling AJ (2010) Investigating soil moisture-climate interactions in a changing climate: a review. *Earth-Sci Rev* 99(3):125–161. <https://doi.org/10.1016/j.earscirev.2010.02.004>
- Seneviratne SI, Nicholls N, Easterling D, Goodess CM, Kanae S, Kossin J, Luo Y, Marengo J, McInnes K, Rahimi M, Reichstein M, Sorteberg A, Vera C, Zhang X (2012) Changes in climate extremes and their impacts on the natural physical environment. In: Field CB, Barros V, Stocker TF, Qin D, Dokken DJ, Ebi KL, Mastrandrea MD, Mach KJ, Plattner G-K, Allen SK, Tignor M, Midgley PM (eds) *Managing the risks of extreme events and disasters to advance climate change adaptation. A special report of working groups I and II of the intergovernmental panel on climate change (IPCC)*. Cambridge University Press, Cambridge, pp 109–230
- Seneviratne SI, Zhang X, Adnan M, Badi W, Dereczynski C, Di Luca A, Ghosh S, Iskandar I, Kossin J, Lewis S, Otto F, Pinto I, Satoh M, Vicente-Serrano SM, Wehner M, Zhou B (2021) Weather and Climate Extreme Events in a Changing Climate. In: Masson-Delmotte V, Zhai P, Pirani A, Connors SL, Péan C, Berger S, Caud N, Chen Y, Goldfarb L, Gomis MI, Huang M, Leitzell K, Lonnoy E, Matthews JBR, Maycock TK, Waterfield T, Yelekçi O, Yu R, Zhou B (eds) *Climate change 2021: The physical science basis. Contribution of working group I to the 6th assessment report of the intergovernmental panel on climate change*. Cambridge University Press, Cambridge, pp 1513–1766. <https://doi.org/10.1017/9781009157896.013>
- Silva MES, Silva CB, Ambrizzi T, Drumond A, Patucci NN (2020) South America climate during the 1970–2001 Pacific Decadal Oscillation phases based on different reanalysis datasets. *Front Earth Sci* 7:2296–6463. <https://www.frontiersin.org/articles/10.3389/feart.2019.00359>
- Taylor KE (2001) Summarizing multiple aspects of model performance in a single diagram. *J Geophys Res* 106(D7):7183–7192. <https://doi.org/10.1029/2000JD900719>
- Tencer B, Weaver A, Zwiers F (2014) Joint occurrence of daily temperature and precipitation extreme events over Canada. *J Appl Meteorol Climatol* 53(2148):2162
- Tencer B, Bettolli M, Rusticucci M (2016) Compound temperature and precipitation extreme events 1 in Southern South America: associated atmospheric circulation and simulations by a multi-RCM ensemble. *Clim Res* 68:183–199
- Trenberth KE, Shea DJ (2005) Relationships between precipitation and surface temperature. *Geophys Res Lett* 32:L14703. <https://doi.org/10.1029/2005GL022760>
- Voltaire A, Saint-Martin D, Sénési S, Decharme B, Alias A, Chevallier M et al (2019) Evaluation of CMIP6 DECK experiments with CNRM-CM6-1. *J Adv Model Earth Syst* 11:2177–2213. <https://doi.org/10.1029/2019MS001683>
- von Storch H, Zwiers F (1999) *Statistical analysis in climate research*. Cambridge University Press, Cambridge. <https://doi.org/10.1017/CBO9780511612336>
- Wang S, Huang J, He Y, Guan Y (2014) Combined effects of the Pacific decadal oscillation and El Niño–Southern oscillation on global land dry–wet changes. *Sci Rep* 4(1):1. <https://doi.org/10.1038/srep06651>
- Whan K, Zscheischler J, Orth R, Shongwe M, Rahimi M, Asare EO, Seneviratne SI (2015) Impact of soil moisture on extreme maximum temperatures in Europe. *Weather Clim Extrem* 9:57–67. <https://doi.org/10.1016/j.wace.2015.05.001>
- Wu X, Hao Z, Zhang X, Li C, Hao F (2020) Evaluation of severity changes of compound dry and hot events in China based on a multivariate multi-index approach. *J Hydrol* 583:124580. <https://doi.org/10.1016/j.jhydrol.2020.124580>
- Xie P, Yatagai A, Chen M, Hayasaka T, Fukushima Y, Liu C, Yang S (2007) A gauge-based analysis of daily precipitation over East Asia. *J Hydrometeorol* 8(607):626
- Yeh S, Kug J, Dewitte B, Kwon M, Kirtman B, Jin F (2009) El Niño in a changing climate. *Nature* 461:511–514
- Zhou P, Liu Z (2018) Likelihood of concurrent climate extremes and variations over China. *Environ Res Lett* 13(9):094023. <https://doi.org/10.1088/1748-9326/aade9e>

- Zscheischler J, Seneviratne SI (2017) Dependence of drivers affects risks associated with compound events. *Sci Adv* 3(6):e1700263. <https://doi.org/10.1126/sciadv.1700263>
- Zscheischler J, Westra S, van den Hurk BJJM, Seneviratne SI, Ward PJ, Pitman A et al (2018) Future climate risk from compound events. *Nat Clim Change* 8:469–477. <https://doi.org/10.1038/s41558-018-0156-3>

Publisher's Note Springer Nature remains neutral with regard to jurisdictional claims in published maps and institutional affiliations.